

One Pot Synthesis and Spectral Analysis of Ag Doped Polyvinyl Pyrrolidone Encapsulated Zinc Oxide Nano Composites and its Antibacterial Efficacy

Saravana Vadivu Arunachalam, Arunpandian. M

Abstract: A facile wet chemical method is used for the preparation of the transition metal doped semiconducting materials. To prepare pure PVP encapsulated ZnO nano particles by taking 1g PVP which was dissolved in 50 ml of ethanol and the solution is stirred for 2 hours at room temperature. After the stirring process zinc nitrate of (0.5, 1.0, 1.5)g was added and to this solution add 0.1g of silver nitrate and stir vigorously. The resultant product is kept aside for ten day, then dried under vacuo and annealed. The synthesized nano material was preserved in an airtight container and it is subjected for various spectral investigation tools like X-Ray Diffraction analysis, High Resolution Scanning Electron microscope Analysis, Photoluminescence studies, Ultra Violet Absorption and Fourier Transform Infrared Spectroscopic studies. The XRD results reveal that the synthesized samples are in highly crystalline in state and also show that the sample does not contain any metal peak which shows that the synthesized samples are in highly pure phase. The HR SEM result shows that the materials are in Nano phase. The UV visible absorption spectroscopic study shows strong absorption peaks of ZnO around 295 nm and Ag doped ZnO around 280 nm which is caused by the band edge transition of the synthesized semiconductor. The FTIR studies are also shows characteristic peaks for PVP, ZnO, Ag doped ZnO nanocomposites. The ZnO nano material behaves as a potential antimicrobial agent but the silver doped ZnO shows a lesser activity while comparing with the standard drug (Streptomycin).

Keywords: PVP encapsulated ZnO, One pot synthesis, Nano phase, Streptomycin, Biological study

I. INTRODUCTION

Recently, major interest has been devoted to the transition metal oxides doped with the different substrates [1]. These materials are good candidates for applications in semiconductors, photocatalysis, sensors, antimicrobial agents and displays [2–8]. Silver and silver-based compounds are well-investigated antimicrobial agents being biocompatible and non-toxic to human cells at concentrations effective against microorganisms when in the form of non-agglomerated and well dispersed nanoparticles [9-12]. In this communication, we are reporting versatile approach to synthesize materials/products that are in powdery form and are very effective as antibacterial agents. We have conducted

investigations on the efficacy of silver-doped product and non-silver doped product. The un-embedded product was also prepared and subjected to the same treatment to serve as reference. A project on further innovative industrial applications of these products is in progress.

II. EXPERIMENTAL DETAILS

Materials and Methods

All the reagents used were analytical reagent grade. Solvents were purified and dried according to the standard procedures.

All the reactions were carried out under anhydrous conditions. Zinc nitrate, Silver nitrate, Polyvinyl pyrrolidone (PVP), ethanol was purchased from Sigma and was used without further purification. The analysis of carbon, hydrogen, nitrogen and sulphur were performed in Vario EL III CHNS analyzer at Cochin University, Kerala, India. IR spectra were recorded as KBr pellets in the 4000-400 cm⁻¹ region using a Shimadzu FT-IR 8000 spectro-photometer. Electronic spectra were recorded in dichloromethane Melting points were recorded on a Veego VMP-DS melting point apparatus and are uncorrected.

To prepare pure PVP encapsulated ZnO nano particles by taking 1g polyvinyl pyrrolidone which was dissolved in 50 ml of ethanol and the solution is stirred for 2 hours at room temperature. After the stirring process zinc nitrate of (0.5, 1.0, 1.5)g was added to the solution and stirred which was completely dissolved into the solution.

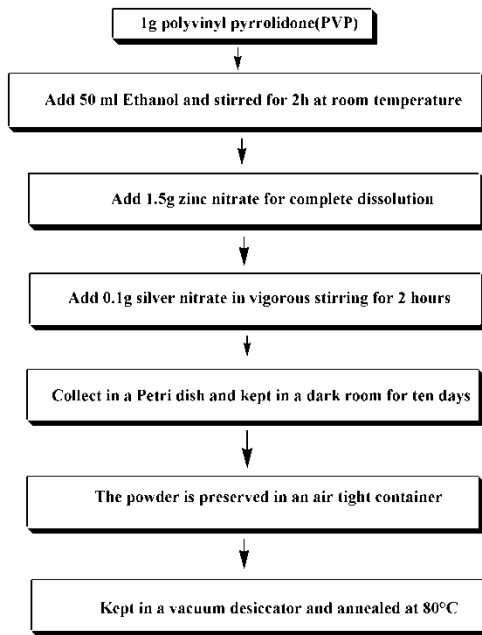
The solution was poured into a Petri dish and kept in a dark room for ten days. Then it can be kept into a vacuum desiccator and then the particles are collected and grained and preserved in an air tight container. The flow chart for the preparation of PVP encapsulated ZnO nano particles is given below,

Revised Manuscript Received on December 05, 2019.

* Correspondence Author

S. Arunachalam*, Nanomaterials Laboratory, Department of Chemistry, International Research Centre, Kalasalingam Academy of Research and Education (Deemed to be University), Krishnankoil – 626126, India. Email: drarunachalam.s@gmail.com

M. Arunpandian, Nanomaterials Laboratory, Department of Chemistry, International Research Centre, Kalasalingam Academy of Research and Education (Deemed to be University), Krishnankoil – 626126, India. Email: arunpandiantl26@gmail.com



Antimicrobial Activity

A smear was prepared on a glass slide using a sterile wire loop and allowed to dry. Fixed the smear by passing the slide rapidly over the flame. Stained it for 1 minute with crystal violet solution and washed it in tap water. Applied the gram’s iodine solution and washed it in tap water after 1 minute. Decolorized with alcohol by adding dropwise on the titled slide. Appile the counter strain for 1 minute, washed and air-dried.

Melted the agar in the tubes while sterilizing, cooled it and keep it at 450 C. Poured about 20 ml of the agar medium into each of the petridishes. Allowed them to cool and labeled the petridishes. Added the required gut sample from the rearing medium into the sterile water in test tubes, shaken the test tubes and allowed to settle. Using a sterilize 1 ml pipette added 1 ml sample each into the plates and spreaded the plate by tilting it back and forth or using a sterile ‘L’ rod. Left a plate as control. Inverted all the plates and incubated them at 300C is an incubator for 2 days, observed different types of colonies.

III. RESULTS AND DISCUSSION

X Ray Diffraction Structural Analysis:

The XRD pattern of PVP (1 gm) encapsulated ZnO (0.5 - 1.5 gm) nanoparticles prepared at room temperature is represented in FIGURE1.a (Tables 1). The sharp diffraction peaks of miller planes (100), (101), (102), (103) indicate the crystalline ZnO hexagonal wurtzite structure, which are agreed well with the standard JCPDS card (21-1272). Intensity of the diffraction peaks enhance with the ZnO concentration in the growth medium.

Further, upon increasing concentration, it shows feeble shift towards the lower angle in their positions. The average particle sizes calculated from the analysis using ‘Debye Scherer’ formula is found to be 15 nm. As the Zn precursor ratio is increased to 1.0 gm, the crystallinity of the materials is also increased. Further raise in the concentration results with formation of multiple faceted orientations [13].

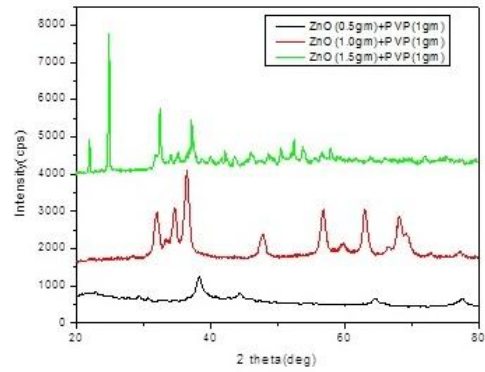


Figure 1.a. XRD pattern of ZnO nanoparticles

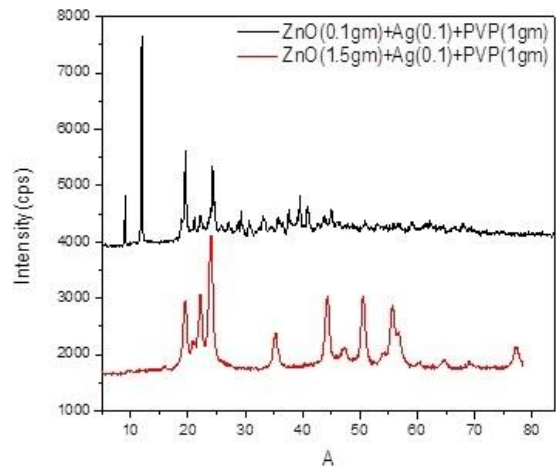


Figure 1.b. XRD pattern of Silver doped ZnO Nanocomposites

Figure1.b shows the XRD spectra of Agdoped ZnO encapsulated with PVP nano composites prepared for low concentration of ZnO nanoparticles are shown in the Figure 5.1(b) which exhibit the presence of hexagonal structured ZnO doped with Ag in the PVP matrix. The figure also shows the prominent peaks at 2θ angles namely 35.89°, 40.82° and 44.93° and are related to the plane values (004), (101), (102) and (103) respectively. The presence of a less intense peak at 35.89° is correlated to the miller plane (004) doped state of low concentrated ZnO present in the PVP matrix. The other peaks are matched with the standard data JCPDS card number (89-0510). The average crystallite size of the doping material is calculated ranged between 15 and 30 nm.

UV VISIBLE SPECTROSCOPY:

The absorption spectra of the ZnO nanostructures dispersed in PVP matrices spread in ethanol solution is shown in figure 2.a. and the results given in the table 2. The band position corresponds to ZnO nanoparticles are blue shifted from their characteristics absorption region due to the size reduction and controlled by PVP materials. The blue shift in the absorption edges is attributed to the quantum confinement of the ZnO nanostructures. Intensity of the absorption edges increases with increased with the Zn concentration and it infers the more formation of ZnO. Further, it supports the XRD results.



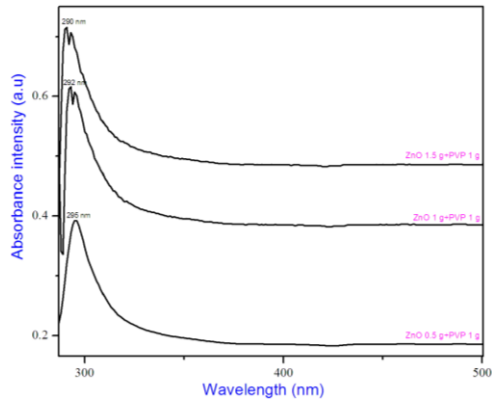


Figure 2.a. Absorption spectra of ZnO nano particle with PVP (1.0 gm)

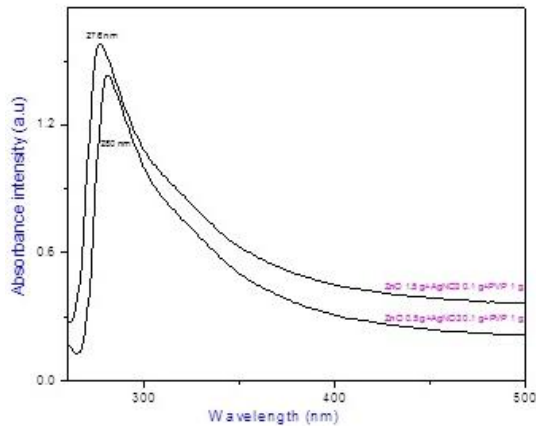


Figure 2.b. UV-Visible spectrum of Silver doped ZnO nanocomposites

The optical properties of PVP encapsulated ZnO nanoparticles are showed in the figure 2.a. and the results given in the table 2. The sharp absorption band at 295 nm is attributed to the monodispersed state of the prepared nanosystems. Band gap energy was calculated from the spectrum which ensemble the increased energy gap which is also further resembled the reduced particle size of the nanoparticles. The sharpness of the absorption edge denotes the less defect particles in the PVP matrices. The PVP encapsulated ZnO nanoparticles (0.5 to 1.5 gm) shows decrease in absorption intensity, due to the increase of ZnO nanoparticles in the PVP matrix. The band gap energy was calculated for high concentration ZnO which shows decreased state due to the increase the concentration of ZnO nanoparticles in the PVP matrix.

The optical properties of PVP encapsulated Silver doped ZnO nanocomposites showed that the absorption peak at 280 nm. The 0.1g Agparticles doped with 0.5gm, 1.5gm of ZnO in the concentration of 1gm PVP matrix. The absorption peak position decreases due to the doping of Agparticle with ZnO nanoparticle in the PVP matrix. The bandgap energy was calculated and it was slightly increasing than the ZnO nanoparticles [14].

PHOTOLUMINESCENCE SPECTROSCOPY:

The photoluminescence spectra of the as prepared pure ZnO nanoparticles are excited at 325 nm and are shown in figure 3.a. A rather broader near band edge emission peak at about 365 nm, a stronger and broad violet emission peak at 540 nm for various concentrations are observed from analysis. In the case of ZnO nanoparticles, It is well reported

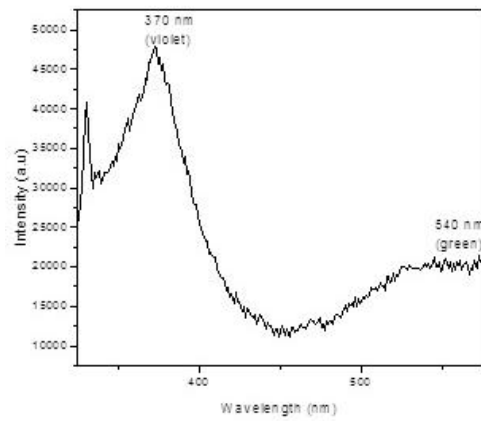


Figure 3.a. UV-Visible spectrum of 1gm PVP+0.5gm ZnO

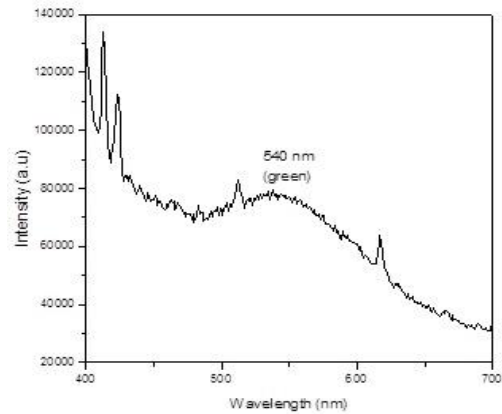


Figure 3.b. UV-Visible spectrum of 1gm PVP+1gm ZnO

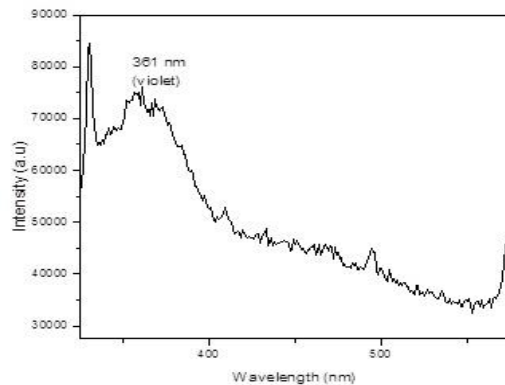


Figure 3.c. UV-Visible spectrum of 1gm PVP+1.5gm ZnO

and expected to receive a stronger deep level emission in the visible region as the function of the concentration. It is further referenced that bulk material show weak luminescence owing to their indirect band gap property. It is also believed that the quantum confinement is also reasoned for the band gap nature was changed from indirect to direct band gap. From the band to band transition, the calculated band gap from the energy - frequency relation $E=h\nu$ and its calculated value is 3.8eV. When being direct band gap for pure material it shows wider photoluminescence was possible. From this result, it is observed that, the quantum confinement effect takes place [15]. The Illustrated figure (3.b and 3.c) shows the photoluminescence spectra of pure ZnO nanocomposites in the PVP matrix were excited at 425nm and 330nm and the emission peaks are obtained at 540nm and 361nm.

It shows near green region and maximum emission intensity were obtained around at 280 nm with very strong and violet emissions are obtained at 361nm. The direct band gap for pure ZnO is 3.5ev.

PL SPECTRUM OF SILVER DOPED ZNO NANOCOMPOSITES

We investigated the emission behavior of the silver doped ZnO nanocomposite with different AgNO₃ concentrations. The photoluminescence from the roughened surface of noble metals could be viewed as an excitation of electrons from occupied d-bands into states above the Fermi level and the similar mechanism is responsible for the nano cluster photo luminescence. Subsequent electron-phonon and hole-phonon scattering process lead to energy loss and finally photo luminescent recombination of an electron from an occupied sp band with the hole. On the other hand, there was no photoluminescence for large metal particles, for this rapid radiation less processes. It has been suggested that the fluorescence from monolayer-protected silver nanoparticles is caused by smaller cluster derived from the interaction between the surface of monolayer protected nanoparticles and the solvent under the exciting light.

Figure(3.d.) &figure(3.e.) shows the photoluminescence spectrum of the silver doped ZnO(0.5g) excited at 300nm, the emission peaks are 375nm and 440nm for blue region and the silver doped ZnO(1.5g) excited at 440nm and the emission peaks are 540nm near green region. The direct band gap for doped material is 2.8 eV.

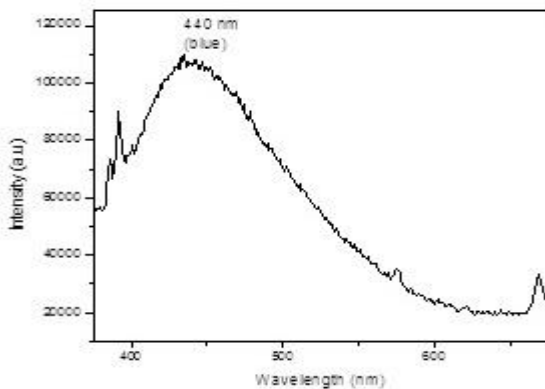


Figure 3.d. UV-Visible spectrum of 1 g PVP + 0.5 g ZnO + 0.5 g Ag

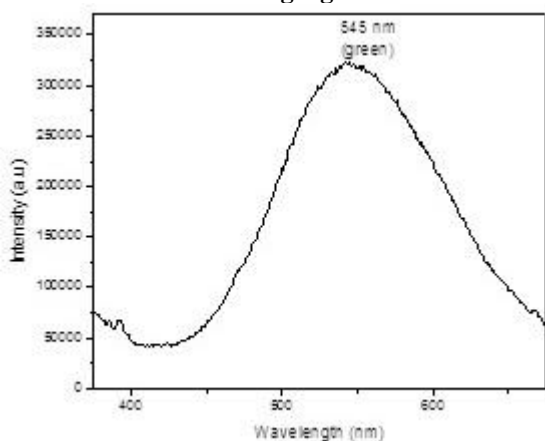


Figure 3.e. UV-Visible spectrum of 1 g PVP + 1.5 g ZnO + 1.5 g Ag

FTIR SPECTROSCOPY:

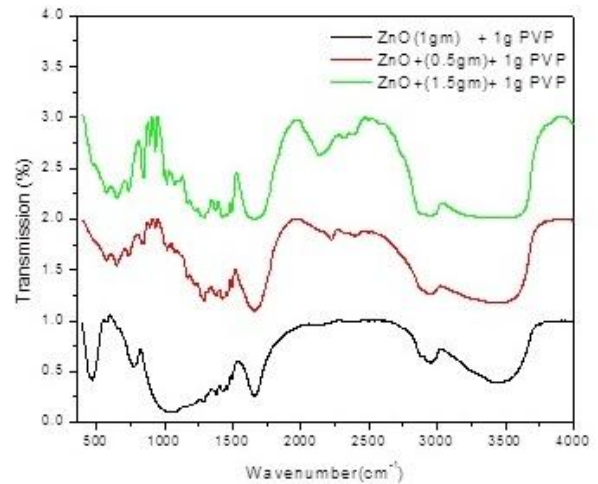


Figure 4.a. FT-IR spectrum of ZnO with PVP Nanoparticles

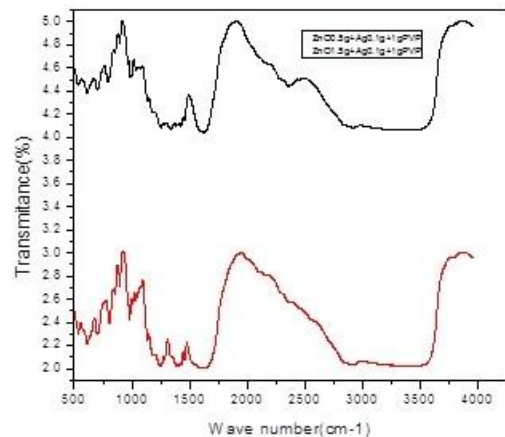


Figure 4.b. FT-IR spectrum of Silver doped ZnO nanocomposites

The natural vibration of atoms in molecules in the infrared ranges which facilities to identify the short range ordering of atoms in a material. Further this technique is to identify the reaction between the solids by monitoring the vibrational and rotational motion of molecules during the reaction. The KBR pellet technique was employed for recording the FTIR spectra using 84005 Shimadzu spectrometer (With the resolution of 3cm-1 in the wavelength range of 3000-3500 cm-1). In fig (4.a.) shows that the broad peak in ZnO nanoparticles. The OH group present in the sample, the peak which is located at 2935cm-1 to 2927cm-1 are due to the symmetric and asymmetric C-H bonds respectively. The C-H bonds are present in mono acetate are intermediate products from 1423cm-1 to 1384cm-1 peaks are attributed to asymmetric and symmetric C=O bonds vibrations respectively. C-N bonds vibrate at 1010cm-1, 1066.61cm-1 and 1234.41cm-1. The OH vibration become sharper and all the vibration moderated due to increase in ZnO concentration. The PVP shifted peak from 1662cm-1-1649cm-1 due to the presence of metal oxide nanoparticle inside the PVP matrix. For various concentrations of metal oxide nanoparticles shows the presence of PVP in low concentration.



The FTIR spectra of Ag/ZnO nanocomposites are provided in fig (4.b.).The peaks at 1658 cm⁻¹ and 1610 cm⁻¹ are attributed to O-H stretching and bending vibrations of water molecules respectively. The band at around 1448 cm⁻¹ was attributed to the vibration mode Ag bond with O, after the addition of Ag on the surface of ZnO nanoparticle the band around 861cm⁻¹ disappear and new band 1251.5cm⁻¹ was formed. The distinct differences between the IR band of Ag/Zno nanocomposites were absorbed between 530 cm⁻¹ and 805 cm⁻¹. The differences of changes indicate that peak addition of Ag affected ZnO nanocomposites. The broad peak at 1621 is sharpened due to increase metal oxide nanoparticle which indicates the presence of PVP matrix. These results were good agreement in the previous report.

SEM ANALYSIS:

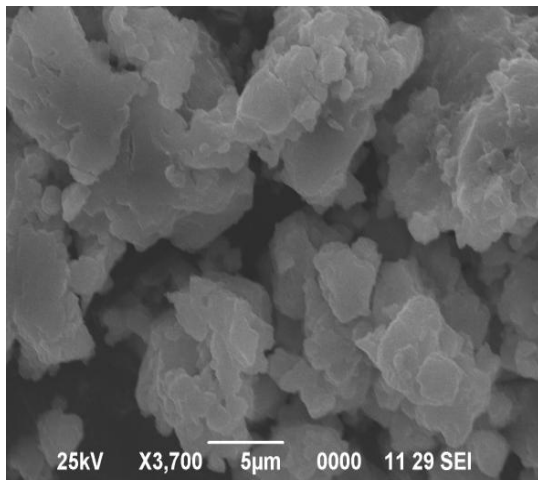


Figure.5.a. SEM image of 1 g PVP+1.5 g ZnO

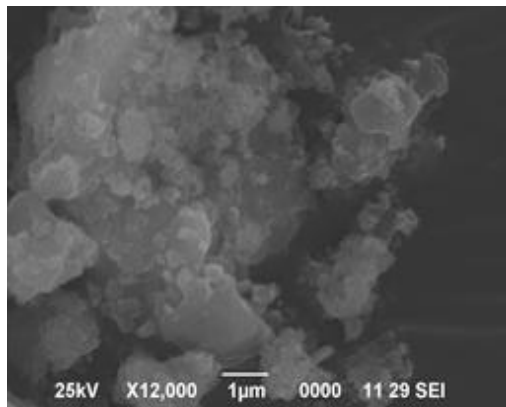


Figure 5.b. SEM image of 1.5 g ZnO + 0.1 g AgNO₃ + 1 g PVP

The morphology analysis of prepared samples was done with scanning electron microscope. Figure (5.a.) shows the SEM images of the as prepared PVP encapsulated ZnO nanoparticles at 5μm magnifications. At low magnification, the formation of plate like structures has been clearly indicated.

Figure (5.b.) shows the SEM images of the PVP encapsulated silver doped ZnO nano composites. From low magnification image clearly view that the particle size and no structure had been clearly seen. The low magnification image was taken as in 1μm clearly shows the formations of the

plates are piled up. The different morphologies were observed. Therefore its considered as a optimized sample for the further analysed.

ANTIMICROBIAL ACTIVITY

From the results it was concluded that the addition of silver doped ZnO nanocomposite into the microorganism damaged it in a lesser rate as compared with pure ZnO nanoparticles. Therefore, these results are helpful to confirm that the silver doped ZnO was very less toxic to living organisms but pure ZnO nanoparticles are suitable for killing effect of bacteria from environment i.e. for anti-microbial activity [16].

From the prepared nanoparticles, 0.5 gm and 1.5 gm of ZnO nanoparticle was taken and diluted in 10 ml of ethanol and kept in ultrasonic agitator for 15 min to get fine dispersion of particles. The diluted ZnO nanoparticles solution was dropped into the grown bacteria and incubated. After 12 hrs, the killing effect of human E.Coli bacteria was examined using fluorescence microscope and the same examination was repeated for after 24 hrs. The taken images (Fig 6.a. and 6.b.) were shown in in which the images corresponding to 12 hr and 24 hrs indicated the killing effect of bacteria after the addition of ZnO and starched capped ZnO nanoparticles [17,18].



Figure. 6.a. Fluorescence image of ZnO 0.1 g + 1 g PVP + 1 g Ag



Figure. 6.b. Fluorescence image of ZnO 1.5 g + 1 g PVP + 1 g Ag

IV. CONCLUSIONS

The simple chemical method is employed for the preparation of the transition metal doped semiconducting materials. The synthesized nano material was preserved in an airtight container and it is subjected for various characterization tools like X-Ray Diffraction analysis, High Resolution Scanning Electron microscope Analysis, Photoluminescence studies, Ultra Violet Absorption and Fourier Transform Infrared Spectroscopic studies.

The XRD results reveal that the synthesized samples are in highly crystalline in state with nano dimensional state. The results also show that the sample does not contain any metal peak which shows that the synthesized samples are in highly pure phase. The HR SEM result shows that the materials are in Nano phase.

The UV visible absorption spectroscopic study shows strong absorption peaks of ZnO around 295 nm and Ag doped ZnO around 280 nm which is caused by the band edge transition of the synthesized semiconductor. The FT IR studies are also shows characteristic peaks for Pure ZnO and Ag doped ZnO nanocomposites. The functional groups peaks are also found in the spectrum and it is attributed as they are in the surface of the final product. The ZnO nano material behaves as a potential antimicrobial agent but the silver doped ZnO shows a lesser activity while comparing with the standard drug (Streptomycin).

REFERENCES

- M. H. Habibi, R. Sheibani, J. Indust. Eng. Chem., 2013, 19, 161–165. b) X.Z. Meng, L. Xiaojing, H.R. Hang, X.H. Yueyue, W. Xiaohong, Y. B. Tang, X. Zhang, M. Li, X. He, R. Hang, X. Huang, Y. Wang, X. Yao, Appl. Sur. Sci., 2015, Article in press.
- A.A. Aal, M.A. Barakat, R.M. Mohamed, Appl. Surf. Sci., 2008, 254, 4577. b) X. L. Cheng, H. Zhao, L. H. Huo, S. Gao, J. G. Zhao, Sens. Actuators B, 2004 102, 248.
- J.Y. Son, S.J. Lim, J.H. Cho, W.K. Seong, H. Kim, Appl. Phys. Lett., 2008, 93, 053109. b) Wnek G E, Carr M E, Simpson D G and Bowlin G L 2003 Nano Lett. 3 213.
- M.H. Cho, G.H. Lee, Thin Solid Films, 2008, 516, 5877. b) M. Singhal, V. Chhabra, P. Kang, D. O. Shah, Material science Res. Bull., 32 (1997) 239-247.
- M.R. Vaezi, J. Mater. Process. Technol., 205 (2008) 332. b) [4] H. Yang, Y. Ji Sun, W. Song, X. Zhu, Y. Yao, Z. Zhang, Corros. Sci. 50 (2008) 3160. c) M.H. Habibi, R. Sheibani, Bull. Environ. Contam. Toxicol. 2010, 85, 589. d) M. Montazerzohori, B. Karami, M.H. Habibi, Ann. Chim. 2006, 285, 5-6. e) M. Montazerzohori, B. Karami, M.H. Habibi, Fresenius Environ. Bull., 2007, 16 44.
- N. Wang, X.Y. Li, Y.X. Wang, Y. Hou, X.J. Zou, G.H. Chen, Mater. Lett., 2008, 62, 3691. b) A. Hilonga, J.K. Kim, P.B. Sarawade, H.T. Kim, Applied Surface Science 2009, 255, 8239. c) A. Hilonga, J.K. Kim, P.B. Sarawade, H.T. Kim, Applied Surface Science 2010, 256, 2849–2855. d) H. Liu, Q. Chen, L. Song, R. Ye, J. Lu, H. Li, Journal of Non-Crystalline Solids, 2008, 354 1314–1317. e) D.V. Quang, P.B. Sarawade, A. Hilonga, S.D. Park, J.K. Kim, H.T. Kim, Applied Surface Science, 2011, 257, 4250–4256.
- L.X. Shi, H. Shen, L.Y. Jiang, X.Y. Li, Mater. Lett., 2007, 61, 4735. b) T. Toshiakazu, Inorganic Materials, 1999, 6, 505–511. c) M. Kawashita, S. Tsuneyama, F. Miyaji, T. Kokubo, H. Kozuka, K. Yamamoto, Biomaterials, 2000, 21, 393. d) L. Miao, P. Jin, K. Kaneko, A. Terai, N. Nabatova-Gabain, S. Tanemura, Applied Surface Science, 2003, 212, 255–263.
- M.H. Habibi, M. Mikhak, Appl. Surf. Sci., 2012, 258, 6745. S.M. Hosseini, b) I. A. Sarsari, P. Kameli, H. Salamati, J. Alloys Compounds, 2015, 640, 408–415. c) A. Tsukazaki, A. Ohtomo, T. Onuma, M. Ohtani, T. Makino, M. Sumiya, K. Ohtani,
- S.F. Chichibu, S. Fuke, Y. Segawa, Nat. Mater., 2004, 4, 42–46. d) U. Ozgur, Y.I. Alivov, C. Liu, A. Teke, M. Reshchikov, S. Dogan, V. Avrutin, S.J. Cho, H. Morkoc, J. Appl. Phys., 2005, 98, 041301. e) M. Ahmad, J. Zhao, J. Iqbal, W. Miao, L. Xie, R. Mo, J. Zhu, J. Phys. D: Appl. Phys., 2009, 42, 165406. f) S.T. Teklemichael, W.H. Oo, M. McCluskey, E.D. Walter, D.W. Hoyt, Appl. Phys. Lett., 2011, 98, 232112.
- D.V. Quang, P.B. Sarawade, A. Hilonga, S.D. Park, J.K. Kim, H.T. Kim, Appl. Surf. Sci., 2011, 257, 4250–4256. b) [12] C. Karunakaran, V. Rajeswari, P. Gomathisankar, Solid State Sci., 2011, 13, 923–928. c) P. Amornpitoksuk, S. Suwanboon, S. Sangkanu, A. Sukhoom, N. Muensit, J. Baltrusaitis, Powd. Technol., 2012, 219, 158–164. d) T. Chen, Y. Zheng, J.-M. Lin, G. Chen, J. Am. Soc. Mass Spectro., 2008, 19, 997–1003.
- D. Gangadharan, K. Harshvardan, G. Gnanasekar, D. Dixit, K.M. Popat, P.S. Anand, Water Research, 2010, 44 5481–5487. b) M. Jelinek, T. Kocourek, J. Remsa, M. Weiserová, K. Jurek, J. Mikššovský, J. Strnad, A. Galandáková, J. Ulřichová, Materials Science and Engineering C, 2013, 33, 1242–1246. c) A.B.G. Lansdown, in: G. Burg (Ed.), Curr Probl. Dermatol, Basel, Karger, 2006. c) Y. Chen, X. Zheng, Y. Xie, Ch. Ding, H. Ruan, C. Fan, J. Mater. Sci. Mater. Med., 2008, 19, 3603–3609. d) W. Chen, Y. Liu, H.S. Courtney, M. Bettenga, C.M. Agrawal, J.D. Bumgardner, J.L. Ong, Biomaterials, 2006, 27, 5512–5517. e) R.J. Chung, M.F. Hsieh, K.C. Huang, L.H. Perng, F.I. Chou, T.S. Chin, J. Sol–Gel Sci. Technol., 2005, 33, 229–239.
- R. Bandyopadhyaya, M.V. Sivaiah, P.A. Shankar, J. Chem. Tech. Biotech., 2008, 83 1177–1180. b) C.F. Koch, S. Johnson, D. Kumar, M. Jelinek, D.B. Chrisey, A. Doraiswamy, C. Jin, R.J. Narayan, I.N. Mihailescu, Mater. Sci. Eng. C, 2007, 27, 484–494. c) R.K. Appleyard, Genetics, 1954, 39, 440–452. c) M. Madigan, J. Martinko, (Eds.), Brock Biology of Microorganisms, 11th Ed., Prentice Hall, 2005. d) S.E. Luria, Cold Spring Harb. Symp. Quant. Biol., 1953, 18, 237–244.
- Y. Lv, H. Liu, Z. Wang, S. Liu, L. Hao, Y. Sang, D. Liu, J. Wang, R.I. Boughton, J. Memb. Sci., 2009, 331 50–56. b) K. SanthoshKumar, A. GowriManohari, S. Dhanapandian, T. Mahalingam, Materials Letters (Article in press). b) A. Akkari, M. Reghima, G. Cathy, N.K. Turki, J. Mater. Sci., 2012, 47 1365–71. c) Y. Yang, S. Cheng, J. Semicond., 2008, 29, 2322–5. d) G. Manohari, D.S. Manoharan, K. Santhosh, T. Mahalingam, Mater. Sci. Semicond. Process., 2014, 17, 138–42. e) D.F. Paraguay, J. Morales, W. Estrada, L. W. Andrade, M.M. Yoshida. Thin Solid Films, 2000, 366, 16–27.
- D. Rajkumar, K. Palanivelu, J. Hazard. Mater., 2004, 113, 123–129. b) H. Noguchi, A. Stiyadi, H. Tanamura, T. Nagatomo, O. Omoto. Sol. Energy. Mater. Sol. Cells, 1994, 35, 325–31. c) M. Ichimura, K. Takeuchi, Y. Ono, E. Arai, Thin Solid Films, 2000, 361, 98–101. d) M.M.E. Nahass, H.M. Zeyada, M.S. Aziz, N.A. El-Ghamaz, Opt. Mater., 2002, 20, 159–70. e) N.K. Reddy, K. Ramesh, R. Ganesan, K.T.R. Reddy, K.R. Gunasekhar, E.S.R. Gopal, Appl. Phys. A, 2006, 83, 133–8.
- D.G. Thomas, J. Phys. Chem. Solids, 1960, 15, 86. b) J. Bardeen, F.J. Blatt, L.H. Hall, Proceeding soft hephotoconductivity conference. Atlantic City, New York, Wiley, 1956; 146. c) T. Minami, T. Kakumu, Y. Takeda, S. Takata. Thin Solid Films, 1996; 290, 1–5. d) G.L. Rusu, M.E. Popa, G.G. Rusu, Appl. Surf. Sci., 2003, 218, 223–31.
- E. Tang, G. Cheng, X. Ma, Powder Technology, 2006, 161, 209–214. b) A. Peetscha, C. Greulich, D. Braun, C. Stroetges, H. Rehaged, B. Siebers, M. Koller, M. Epple, Colloids and Surfaces B: Biointerfaces, 2013, 102, 724–729. c) A.I. Hidron, J.R. Edwards, J. Patel, T.C. Horan, D.M. Sievert, D.A. Pollock, S.K. Fridkin, Infect. Control Hosp. Epidemiol., 2008, 29, 996–1011. c) S.R. Harris, E.J. Feil, M.G. Holden, M.A. Quail, E.K. Nickerson, N. Chantratita, S. Gardete, A. Tavares, N. Day, J.A. Lindsay, J.D. Edgeworth, H. de Lencastre, J. Parkhill, S.J. Peacock, S.D. Bentley, Science, 2010, 327, 469–474. d) C.G. Giske, D.L. Monnet, O. Cars, Y. Carmeli, Antimicrob. Agents Chemother., 2008, 52, 813–821. e) M.A. Fischbach, C.T. Walsh, Science 325 (2009) 1089–1093.
- G. Carotenuto, G. P. Pepe and L. Nicolais. Eur. Phys. J. B, 2007, 16, 11-17. b) R.K. Tamrakar, I.P. Sahu, C.S. Robinson, D.P. Bisen, K. Uplop, Journal of Taibah University for Science., 2015 (Article in Press).
- A.I. Vogel. "Text book of Practical Organic Chemistry", 5th edn Longmann London 1989, 264.
- S. Arunachalam, N. Padma Priya, C. Saravanakumar, C. Jayabalakrishnan, V. Chinnusamy, J. Coord. Chem., 2010, 63, 1795-1806. b) S. Arunachalam, N. Padma Priya, K. Boopathi, C. Jayabalakrishnan, V. Chinnusamy, Appl. Organomet. Chem., 2010, 24, 491-498.

AUTHORS PROFILE



Dr. S. Arunachalam is Assistant Professor in Department of Chemistry, International Research Centre, Kalasalingam Academy of Research and Education (Deemed to be University), Krishnankoil, India. His area of Research is Inorganic and Bio-inorganic chemistry, Photocatalysis, etc.



M. Arunpandian is a research scholar at Nanomaterial Laboratory, Department of Chemistry, International Research Centre, Kalasalingam Academy of Research and Education (Deemed to be University), Krishnankoil, India. He is working in the area materials Characterization, waste water purification and Photocatalysis.